

# ON MODULI OF RINGS AND QUADRILATERALS: ALGORITHMS AND EXPERIMENTS

HARRI HAKULA, ANTTI RASILA, AND MATTI VUORINEN

ABSTRACT. Moduli of rings and quadrilaterals are frequently applied in geometric function theory, see e.g. the Handbook by Kühnau. Yet their exact values are known only in a few special cases. Previously, the class of planar domains with polygonal boundary has been studied by many authors from the point of view of numerical computation. We present here a new *hp*-FEM algorithm for the computation of moduli of rings and quadrilaterals and compare its accuracy and performance with previously known methods such as the Schwarz-Christoffel Toolbox of Driscoll and Trefethen.

FILE: hrv.tex, 2009-07-01, printed: 2022-4-11, 7.13

## 1. INTRODUCTION

Plane domains whose boundaries consist of piecewise-smooth curves occur in applications to electronics circuit design, airfoil modelling in computational fluid dynamics, computer vision and various other problems of engineering and science [21, 22, 23, 27, 30, 32]. In order to specify the shape of the domain we assume that the domain is bounded and that there are either one or two simple (and nonintersecting) boundary curves. The domain is then either simply or doubly connected. For the mathematical modelling of these domains it is usually convenient to map the domains conformally onto “canonical domains” as simple as possible: the unit disk  $\mathbb{D} = \{z \in \mathbb{C} : |z| < 1\}$  or the annulus  $\{z \in \mathbb{C} : r < |z| < 1\}$ . Sometimes a rectangle is more preferable than the unit disk as a canonical domain. The existence of these canonical conformal mappings is guaranteed by classical results of geometric function theory but the construction of this mapping in a concrete application case is usually impossible. Therefore one has to resort to numerical conformal mapping methods for which there exists an extensive literature [17, 23, 26, 30]. The Schwarz-Christoffel (SC) Toolbox of Driscoll [16], based on the software of Trefethen [34], is in wide use for numerical conformal mapping applications.

In the doubly connected case, one might be interested in only knowing the inner radius  $r$  of the canonical annulus. For instance this occurs if we wish to compute the electric resistance of a ring condenser. In this situation the conformal mapping itself is not needed if we are able to find the inner radius  $r$  by some other method. It is a classical fact that the inner radius  $r$  can be obtained in terms of the solution of the Dirichlet problem for the Laplace equation in the original domain with the boundary value 0 on one boundary component and the boundary value 1 on the other one.

---

1991 *Mathematics Subject Classification.* 65E05, 31A15, 30C85.

*Key words and phrases.* conformal capacity, conformal modulus, quadrilateral modulus, *hp*-FEM, numerical conformal mapping.

This fact is just one way of saying that the modulus of a ring domain is conformally invariant: for the canonical annulus  $\{z \in \mathbb{C} : r < |z| < 1\}$  the modulus is equal to  $\log(1/r)$ . This idea reduces the problem of computing the number  $r$  to the problem of numerical approximation of the solutions of Laplace equation in ring domains. In the paper [9] this method was applied to several concrete examples of ring domains for which numerical results were reported, too.

We next consider the case of simply connected plane domains. For such a domain  $D$  and for a quadruple  $\{z_1, z_2, z_3, z_4\}$  of its boundary points we call  $(D; z_1, z_2, z_3, z_4)$  a quadrilateral if  $z_1, z_2, z_3, z_4$  occur in this order when the boundary curve is traversed in the positive direction. The points  $z_k, k = 1, \dots, 4$ , are called the vertices and the part of the oriented boundary between two successive vertices such as  $z_1$  and  $z_2$  is called a boundary arc  $(z_1, z_2)$ . The modulus  $M(D; z_1, z_2, z_3, z_4)$  of the quadrilateral  $(D; z_1, z_2, z_3, z_4)$  is defined to be the unique  $h > 0$  for which there exists a conformal mapping of  $D$  onto the rectangle with vertices  $1 + ih, ih, 0, 1$  such that the points  $z_1, z_2, z_3, z_4$  correspond to the vertices in this order. This conformal mapping is called the canonical conformal mapping associated with the quadrilateral. As in the case of doubly connected domains discussed above, it is well-known that the computation of the modulus  $h$  of the quadrilateral may be reduced to solving the Dirichlet-Neumann boundary value problem in the original domain  $D$  with the Dirichlet boundary values 1 on the boundary arc  $(z_1, z_2)$  and 0 on the arc  $(z_3, z_4)$  and Neumann boundary values 0 on the arcs  $(z_3, z_4)$  and  $(z_4, z_1)$ .

An outline of the structure of this paper now follows. First, in Section 2 we describe the methods used in this paper. In Section 3 we discuss in detail the various FEM methods used here, in particular the  $hp$ -method which was implemented and applied to generate some of the results reported below. Another method we use is the  $h$ -adaptive software package AFEM of K. Samuelsson, which implements an adaptive FEM method and which was previously used in [9]. In the present paper we use the AFEM method to compute the modulus of a quadrilateral whereas in [9] it was used merely for the computation of the moduli of ring domains. In Section 4 a test problem for quadrilaterals is described together with its analytic solution, following [20]. This analytic solution requires, however, an application of a numerical root finding program. Accordingly, this formula is analytic-numeric in its character. In Section 5 we check several methods against this analytic formula in a test involving a family of convex quadrilaterals. The methods discussed are the analytic formula from [20], the Schwarz-Christoffel Toolbox of [16, 17], the AFEM method of Samuelsson [9] and the present  $hp$ -method. On the basis of these experiments, an accuracy ranking of the methods is given in Section 5. In Section 6 the more general case of polygonal quadrilaterals is investigated, in particular L-shaped domains, and the results are compared to the literature. A general observation about the literature seems to be that reported numerical values of the moduli of concrete quadrilaterals (or ring domains) are hard to find in the literature. Perhaps the longest list of numerical results is given in [9] where pointers to earlier literature may be found. The recent book [26] lists also many such numerical values. In our opinion a catalogue of these numerical values in the simplest cases would be desirable for instance for reference

purposes. The book [30] and the paper [27, p. 127] list certain engineering formulas which have been applied in VLSI circuit design.

## 2. METHODS

The following problem is known as the *Dirichlét-Neumann problem*. Let  $D$  be a region in the complex plane whose boundary  $\partial D$  consists of a finite number of regular Jordan curves, so that at every point, except possibly at finitely many points, of the boundary a normal is defined. Let  $\partial D = A \cup B$  where  $A, B$  both are unions of Jordan arcs. Let  $\psi_A, \psi_B$  be a real-valued continuous functions defined on  $A, B$ , respectively. Find a function  $u$  satisfying the following conditions:

- (1)  $u$  is continuous and differentiable in  $\overline{D}$ .
- (2)  $u(t) = \psi_A(t)$ , for all  $t \in A$ .
- (3) If  $\partial/\partial n$  denotes differentiation in the direction of the exterior normal, then

$$\frac{\partial}{\partial n} u(t) = \psi_B(t), \quad \text{for all } t \in B.$$

**2.1. Modulus of a quadrilateral and Dirichlét integrals.** One can express the modulus of a quadrilateral  $(D; z_1, z_2, z_3, z_4)$  in terms of the solution of the Dirichlét-Neumann problem as follows. Let  $\gamma_j, j = 1, 2, 3, 4$  be the arcs of  $\partial D$  between  $(z_4, z_1), (z_1, z_2), (z_2, z_3), (z_3, z_4)$ , respectively. If  $u$  is the (unique) harmonic solution of the Dirichlét-Neumann problem with boundary values of  $u$  equal to 0 on  $\gamma_2$ , equal to 1 on  $\gamma_4$  and with  $\partial u/\partial n = 0$  on  $\gamma_1 \cup \gamma_3$ , then by [1, p. 65/Thm 4.5]:

$$(2.2) \quad \mathbf{M}(D; z_1, z_2, z_3, z_4) = \int_D |\nabla u|^2 dm.$$

**2.3. Modulus of a ring domain and Dirichlét integrals.** Let  $E$  and  $F$  be two disjoint compact sets in the extended complex plane  $\overline{\mathbb{C}}$ . Then one of the sets  $E, F$  is bounded and without loss of generality we may assume that it is  $E$ . If both  $E$  and  $F$  are connected and the set  $R = \overline{\mathbb{C}} \setminus (E \cup F)$  is connected, then  $R$  is called a *ring domain*. In this case  $R$  is a doubly connected plane domain. The *capacity* of  $R$  is defined by

$$\text{cap } R = \inf_u \int_R |\nabla u|^2 dm,$$

where the infimum is taken over all nonnegative, piecewise differentiable functions  $u$  with compact support in  $R \cup E$  such that  $u = 1$  on  $E$ . It is well-known that the harmonic function on  $R$  with boundary values 1 on  $E$  and 0 on  $F$  is the unique function that minimizes the above integral. In other words, the minimizer may be found by solving the Dirichlét problem for the Laplace equation in  $R$  with boundary values 1 on the bounded boundary component  $E$  and 0 on the other boundary component  $F$ . A ring domain  $R$  can be mapped conformally onto the annulus  $\{z : e^{-M} < |z| < 1\}$ , where  $M = \mathbf{M}(R)$  is the *conformal modulus* of the ring domain  $R$ . The modulus and capacity of a ring domain are connected by the simple identity  $\mathbf{M}(R) = 2\pi/\text{cap } R$ . For more information on the modulus of a ring domain and its applications in complex analysis the reader is referred to [1, 21, 22, 26].

In [26, Chapter 3] N. Papamichael describes so called domain decomposition method for the computation of the modulus of a quadrilateral which is designed

to the case of elongated quadrilaterals and applies e.g. to polygonal quadrilaterals that can be decomposed into simple pieces whose moduli can be estimated. As an example he considers a spiraling quadrilateral that can be decomposed into a "sum" of 13 trapezoids and reports results that are expected to be correct up to 7 decimal places. Therefore, this method seems very attractive for the computation of the modulus of a special class of quadrilaterals. A key feature of the method is that it reduces the numerical difficulties caused by the crowding phenomenon for this special class of quadrilaterals.

**2.4. Classification of methods for numerical computing.** For the computation of the modulus of a quadrilateral or of a ring domain there are two natural approaches

- (1) methods based on the definition of the modulus and on the use of a conformal mapping onto a canonical rectangle or annulus,
- (2) methods that give only the modulus, not the canonical conformal map.

In some sense, methods of class (1) give a lot of extra information, namely the conformal mapping – all we want is a single real number. Methods of class (2) rely on solving the Dirichlet-Neumann boundary value problem or Dirichlet problem for the Laplace equation as described above.

In this paper we will mainly use methods of type (2) that make use of adaptive FEM methods for solving the Laplace equation.

**2.5. Review of the literature on numerical conformal mapping.** With the exception of a few special cases, both of the above methods lead to extensive numerical computation. For both classes of methods there are several options in the literature, see for instance the bibliography of [9]. Various aspects of the theory and practice of numerical conformal mapping are reviewed in the monographs [17, 26, 23, 30]. See also the authoritative surveys [19, 25, 35, 36].

Recently numerical conformal mappings have been studied from various points of view and in various applications by many authors, see e.g. [2, 6, 12, 13, 14, 24, 28, 29].

**2.6. Crowding phenomenon.** The so called crowding phenomenon is a well-documented difficulty in numerical conformal mapping discussed by several authors. The underlying difficulties become clear when considering the conformal mapping of an elongated rectangle onto the unit disk. The difficulties are so severe that the total failure of the numerical procedure may result. For example, considering the quadrilateral  $(Q; 1 + ih, ih, 0, 1)$  and its conformal map  $f$  onto the unit disk with  $f(1 + ih) = -f(0)$ ,  $f(ih) = -f(1)$  we have that the minimal distance of the image points  $f(1 + ih), f(ih), f(0), f(1)$  is less than  $3.4 \cdot 10^{-16}$  for  $h = 1/24$  by [26, p. 132]. Due to the constraints of the floating point arithmetic, it is difficult to even sort the image points in the right order.

Very recently, L. Banjai [6] has devised some methods to alleviate the difficulties caused by the crowding at least in some cases.

### 3. $p$ -, AND $hp$ -FINITE ELEMENT METHOD

In the paper [9] the modulus of a ring domain was computed with the help of the software package AFEM of K. Samuelsson, based on an  $h$ -adaptive finite element

method. It may be easily applied to compute the modulus of a quadrilateral, too, and some results will be reported below. Here the AFEM package will be adopted also to compute the modulus of a quadrilateral.

In this section we describe the high-order  $p$ -, and  $hp$ -finite element methods and report the results of numerical computation of the moduli of a number of quadrilaterals. The paper of Babuška and Suri [5] gives an accessible overview of the method, for a more detailed exposition we refer to Schwab [31], and for those familiar with engineering approach the book by Szabo and Babuška [5] is recommended.

In the  $h$ -version or standard finite element method, the unknowns or degrees of freedom are associated with values at specified locations of the discretization of the computational domain, that is, the nodes of the mesh. In the  $p$ -method, the unknowns are coefficients of some polynomials that are associated with topological entities of the elements, nodes, sides, and interior. Thus, in addition to increasing accuracy through refining the mesh, we have an additional refinement parameter, the polynomial degree  $p$ .

Let us next define a  $p$ -type quadrilateral element. The construction of triangles is similar and can be found from the references given above.

**3.1. Shape functions.** Many different selections of shape functions are possible. We follow Szabo and Babuška [33] and present the so-called hierarchic shape functions.

Legendre polynomials of degree  $n$  can be defined using a recursion formula

$$(3.2) \quad (n+1)P_{n+1}(x) - (2n+1)xP_n(x) + nP_{n-1}(x) = 0, \quad P_0(x) = 1.$$

The derivatives can similarly be computed using a recursion

$$(3.3) \quad (1-x^2)P'_n(x) = -nxP_n(x) + nP_{n-1}(x).$$

For our purposes the central polynomials are the integrated Legendre polynomials

$$(3.4) \quad \phi_n(\xi) = \sqrt{\frac{2n-1}{2}} \int_{-1}^{\xi} P_{n-1}(t) dt, \quad n = 0, 1, \dots$$

which can be rewritten as linear combinations of Legendre polynomials

$$(3.5) \quad \phi_n(\xi) = \frac{1}{\sqrt{2(2n-1)}} (P_n(\xi) - P_{n-2}(\xi)), \quad n = 0, 1, \dots$$

The normalizing coefficients are chosen so that

$$(3.6) \quad \int_{-1}^1 \frac{d\phi_i(\xi)}{d\xi} \frac{d\phi_j(\xi)}{d\xi} d\xi = \delta_{ij}, \quad i, j \geq 2.$$

We can now define the shape functions for a quadrilateral reference element. The shape functions are divided into three categories: nodal shape functions, side modes, and internal modes.

**3.7. Nodal shape functions.** There are four nodal shape functions.

$$\begin{aligned} N_1(\xi, \eta) &= \frac{1}{4}(1 - \xi)(1 - \eta), \\ N_2(\xi, \eta) &= \frac{1}{4}(1 + \xi)(1 - \eta), \\ N_3(\xi, \eta) &= \frac{1}{4}(1 + \xi)(1 + \eta), \\ N_4(\xi, \eta) &= \frac{1}{4}(1 - \xi)(1 + \eta). \end{aligned}$$

Taken alone, these shapes define the standard four-node quadrilateral finite element.

**3.8. Side shape functions.** There are  $4(p-1)$  side modes associated with the sides of a quadrilateral ( $p \geq 2$ ).

$$\begin{aligned} N_i^{(1)}(\xi, \eta) &= \frac{1}{2}(1 - \eta)\phi_i(\xi), \quad i = 2, \dots, p, \\ N_i^{(2)}(\xi, \eta) &= \frac{1}{2}(1 + \xi)\phi_i(\eta), \quad i = 2, \dots, p, \\ N_i^{(3)}(\xi, \eta) &= \frac{1}{2}(1 + \eta)\phi_i(\eta), \quad i = 2, \dots, p, \\ N_i^{(4)}(\xi, \eta) &= \frac{1}{2}(1 - \xi)\phi_i(\xi), \quad i = 2, \dots, p. \end{aligned}$$

**3.9. Internal shape functions.** For the internal modes we have two options. The so-called trunk space has  $(p-2)(p-3)/2$  shapes

$$(3.10) \quad N_k^0(\xi, \eta) = \phi_i(\xi)\phi_j(\eta), \quad i, j \geq 2, \quad i + j = 4, 5, \dots,$$

whereas the full space has  $(p-1)(p-1)$  shapes

$$(3.11) \quad N_k^0(\xi, \eta) = \phi_i(\xi)\phi_j(\eta), \quad i = 2, \dots, p, \quad j = 2, \dots, p,$$

where in both cases the index  $k$  depends on the chosen convention. In this paper we always use the full space. The internal shape functions are often referred to as bubble-functions.

**3.12. Parity problem.** The Legendre polynomials have the property  $P_n(-x) = (-1)^n P_n(x)$ . In 2D all internal edges of the mesh are shared by two different elements. We must ensure that each edge has the same global parameterization in both elements. This additional book-keeping is not necessary in the standard  $h$ -FEM.

**3.13. Resource requirements.** We have seen that the number of unknowns in a  $p$ -type quadrilateral is  $(p+2)(p+3)/2$  or  $4p + (p-1)^2$  if the internal modes are from trunk or full space, respectively. To compensate this, the number of elements is naturally taken to be as small as possible. Indeed, when the mesh is adapted in a suitable way, the dimension of the overall linear system can be significantly lower than in the corresponding  $h$ -method. However, the matrices tend to be denser in the

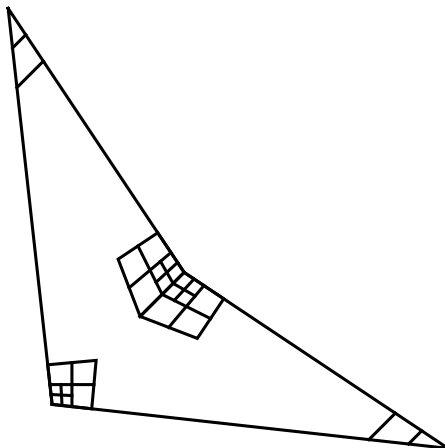


FIGURE 1. Geometric mesh for a general quadrilateral

$p$ -method, so the space requirements in relation to the dimension of the linear system are greater for the  $p$ -method.

**3.14. Proper grading of the meshes** For a certain class of problems it can be shown that if the mesh and the elemental degrees have been set optimally, we can obtain *exponential convergence*. A geometric mesh is such that each successive layer of elements changes in size with some geometric factor, *scaling factor*  $\alpha$ , toward some point of interest. In this case, the points of interest are always corner points.

The following theorem is due to Babuška and Guo [7]. Note that construction of appropriate spaces is technical. For rigorous treatment of the theory involved see Schwab [31], Babuška and Guo [8] and references therein.

**3.15. Theorem.** *Let  $\Omega \subset \mathbb{R}^2$  be a polygon,  $v$  the FEM-solution, and let the weak solution  $u_0$  be in a suitable countably normed space where the derivatives of arbitrarily high order are controlled. Then*

$$\inf_v \|u_0 - v\|_{H^1(\Omega)} \leq C \exp(-b\sqrt[3]{N}),$$

where  $C$  and  $b$  are independent of  $N$ , the number of degrees of freedom. Here  $v$  is computed on a proper geometric mesh, where the orders of individual elements depend on their originating layer, such that highest layers have smallest orders.

*Result also holds for constant polynomial degree distribution.*

Let us denote the number of highest layer with  $\nu$ , the *nesting level*. Using this notation we can refer to geometric meshes as  $(\alpha, \nu)$ -meshes.

In Figure 1 we show a geometric mesh template for a non-convex quadrilateral. Here we require that each node lies at the end point of an edge and so are content if the lines follow the guidelines of the geometric meshes.

In Figure 2 a sequence of real  $p$ -type meshes is shown. The template mesh serves also as a pure  $p$ -type mesh where the approximation properties are changed only by varying the polynomial degree. In the following two meshes the number of elements is the same because the nesting level is the same, only the scaling factor changes.

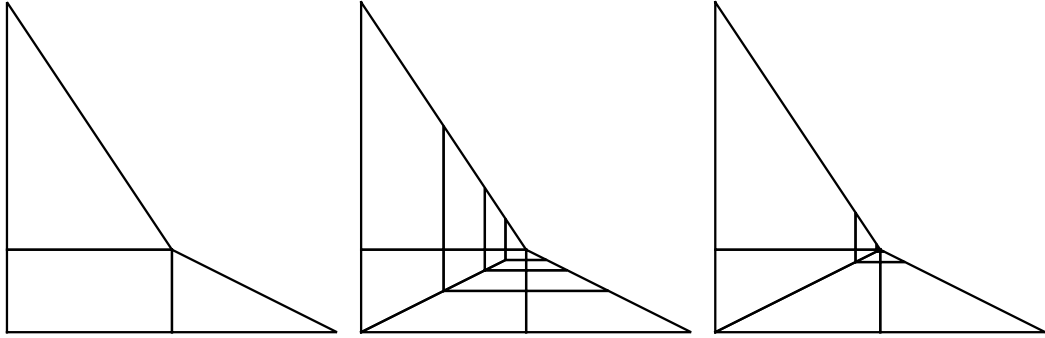


FIGURE 2. Graded meshes: Effect of the scaling factor. From left to right, template mesh,  $(\alpha, \nu) = (1/2, 3)$ ,  $(\alpha, \nu) = (1/6, 3)$ .

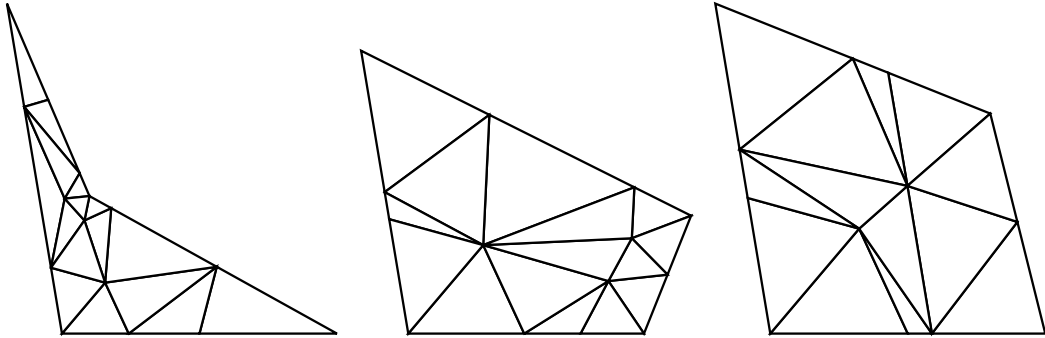


FIGURE 3. Three sample meshes used in numerical experiments below. Note the triangles isolating the corners.

**3.16. Generating geometric meshes.** Here we consider generation of geometric meshes in polygonal domains. We use the following two-phase algorithm:

- (1) Generate a minimal mesh (triangulation) where the corners are isolated with a fixed number of triangles depending on the interior angle,  $\theta$ :
  - $\theta \leq \pi/2$ : one triangle,
  - $\pi/2 < \theta \leq \pi$ : two triangles, and
  - $\pi < \theta$ : three triangles.
- (2) Every triangle attached to a corner is replaced by a refinement, where the edges incident to the corner are split as specified by the scaling factor  $\alpha$ . This process is repeated recursively until the desired nesting level  $\nu$  is reached. Note that the mesh may include quadrilaterals after refinement.

In Figure 3 three minimal meshes and in Figure 4 one final mesh are shown.

#### 4. CONVEX QUADRILATERAL

In this section our goal is to introduce a test problem, whose solution is determined by a transcendental equation. This equation can be numerically solved to the desired accuracy and we will use this to check the validity of the numerical methods we use as well as to obtain an experimental estimate for their accuracy. The test problems we consider are convex polygonal quadrilaterals. The simplest

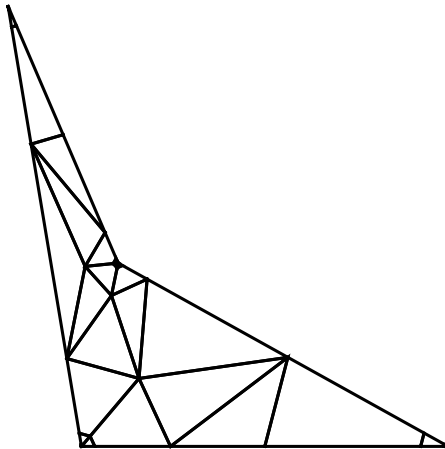


FIGURE 4. Final geometric or  $(0.15, 12)$ -mesh. Due to small  $\alpha$  only first two levels are visible.

such quadrilateral consists of the four vertices and the line segments joining the vertices. Let  $z_1, z_2, z_3, z_4 \in \mathbb{C}$  be distinct points and suppose that the polygonal line that results from connecting these points by segments in the order  $z_1, z_2, z_3, z_4, z_1$  forms the positively oriented boundary of a domain  $Q$ . For simplicity, we denote by  $\text{QM}(z_1, z_2, z_3, z_4)$  the modulus  $M(Q; z_1, z_2, z_3, z_4)$ . Then the modulus is a conformal invariant in the following sense: If  $f: Q \rightarrow fQ$  is a conformal mapping onto a Jordan domain  $fQ$ , then  $f$  has a homeomorphic extension to the closure  $\bar{Q}$  (also denoted by  $f$ ) and

$$M(Q; z_1, z_2, z_3, z_4) = M(fQ; f(z_1), f(z_2), f(z_3), f(z_4)).$$

It is clear by geometry that the following reciprocal identity holds:

$$(4.1) \quad M(Q; z_1, z_2, z_3, z_4)M(Q; z_2, z_3, z_4, z_1) = 1.$$

If  $h: \mathbb{C} \rightarrow \mathbb{C}$  is a translation, rotation, or stretching, then the piecewise linear nature of the boundary is preserved and we can write the conformal invariance simply as

$$\text{QM}(z_1, z_2, z_3, z_4) = \text{QM}(f(z_1), f(z_2), f(z_3), f(z_4)).$$

There are two particular cases, where we can immediately give  $\text{QM}(z_1, z_2, z_3, z_4)$ . The first case occurs, when all the sides are of equal length (i.e. the quadrilateral is a rhombus) and in this case the modulus is 1, see [20]. In the second case  $(Q; z_1, z_2, z_3, z_4)$  is  $(Q; 1 + ih, ih, 0, 1)$ ,  $h > 0$ , and  $\text{QM}(1 + ih, ih, 0, 1) = h$ .

**4.2. Basic identity.** In [20, 2.11] some identities satisfied by the function  $\text{QM}(a, b, 0, 1)$  were pointed out. We will need here the following one, which is the basic reciprocal identity (4.1) rewritten for the expression  $\text{QM}$  :

$$(4.3) \quad \text{QM}(a, b, 0, 1) \cdot \text{QM}((b-1)/(a-1), 1/(1-a), 0, 1) = 1.$$

We shall consider here the following particular cases of this reciprocal identity: (a) parallelogram, (b) trapezoid with angles  $(\pi/4, 3\pi/4, \pi/2, \pi/2)$ , and (c) a convex polygonal quadrilateral. Note that for the cases (a) and (b) the formula is less complex than for the general case (c).

**4.4. The hypergeometric function and complete elliptic integrals.** Given complex numbers  $a, b$ , and  $c$  with  $c \neq 0, -1, -2, \dots$ , the *Gaussian hypergeometric function* is the analytic continuation to the slit plane  $\mathbb{C} \setminus [1, \infty)$  of the series

$$(4.5) \quad F(a, b; c; z) = {}_2F_1(a, b; c; z) = \sum_{n=0}^{\infty} \frac{(a, n)(b, n)}{(c, n)} \frac{z^n}{n!}, \quad |z| < 1.$$

Here  $(a, 0) = 1$  for  $a \neq 0$ , and  $(a, n)$  is the *shifted factorial function* or the *Appell symbol*

$$(a, n) = a(a+1)(a+2) \cdots (a+n-1)$$

for  $n \in \mathbb{N} \setminus \{0\}$ , where  $\mathbb{N} = \{0, 1, 2, \dots\}$  and the *elliptic integrals*  $\mathcal{K}(r), \mathcal{K}'(r)$  are defined by

$$\mathcal{K}(r) = \frac{\pi}{2} F(1/2, 1/2; 1; r^2), \quad \mathcal{K}'(r) = \mathcal{K}(r'), \quad \text{and } r' = \sqrt{1-r^2}.$$

Some basic properties of these functions can be found in [4].

**4.6. Parallelogram.** For  $t \in (0, \pi)$  and  $h > 0$  let

$$g(t, h) \equiv \text{QM}(1 + he^{it}, he^{it}, 0, 1).$$

An analytic expression for this function has been given in [3, 2.3]:

$$(4.7) \quad g(t, h) = \mathcal{K}'(r_{t/\pi}) / \mathcal{K}(r_{t/\pi}),$$

where

$$(4.8) \quad r_a = \mu_a^{-1} \left( \frac{\pi h}{2 \sin(\pi a)} \right), \quad \text{for } 0 < a \leq 1/2,$$

and the decreasing homeomorphism  $\mu_a: (0, 1) \rightarrow (0, \infty)$  is defined by

$$(4.9) \quad \mu_a(r) \equiv \frac{\pi}{2 \sin(\pi a)} \frac{F(a, 1-a; 1; 1-r^2)}{F(a, 1-a; 1; r^2)}.$$

**4.10. Theorem.** [20] *Let  $0 < a, b < 1$ ,  $\max\{a+b, 1\} \leq c \leq 1 + \min\{a, b\}$ , and let  $Q$  be the quadrilateral in the upper half plane  $\mathbb{H} = \{z \in \mathbb{C} : \text{Im } z > 0\}$  with vertices  $0, 1, A$  and  $B$ , the interior angles at which are, respectively,  $b\pi, (c-b)\pi, (1-a)\pi$  and  $(1+a-c)\pi$ . Then the conformal modulus of  $Q$  is given by*

$$\text{QM}(A, B, 0, 1) \equiv \text{M}(Q) = \mathcal{K}(r') / \mathcal{K}(r),$$

where  $r \in (0, 1)$  satisfies the equation

$$(4.11) \quad A - 1 = \frac{Lr'^{2(c-a-b)} F(c-a, c-b; c+1-a-b; r'^2)}{F(a, b; c; r^2)},$$

say, and

$$L = \frac{B(c-b, 1-a)}{B(b, c-b)} e^{(b+1-c)i\pi}.$$

For a fixed complex number  $b$  with  $\text{Im}(b) > 0$  define the following function  $g(x, y) = \text{QM}(x + i \cdot y, b, 0, 1)$  for  $x \in \mathbb{R}$ ,  $y > 0$ . This is well-defined only if the polygonal domain with vertices  $x + i \cdot y$ ,  $b$ ,  $0$ ,  $1$  is positively oriented. This holds e.g. if  $\text{Re}(b) < 0$  and  $x > 0$ . It is a natural question to study the level sets of the function  $g$ . This function tells us how the modulus of a polygonal quadrilateral changes when three vertices are kept fixed and the fourth one is moving. For instance, it was shown in [18] that the function decreases when we move the fourth vertex into certain directions.

**4.12. Trapezoid (Burnside [11]).** In [9, pp. 237-239] so called square frame, the domain between two concentric squares with parallel sides, was considered. Such a domain can be split into 8 similar quadrilaterals, and we shall study here one such quadrilateral with vertices  $1 + hi$ ,  $(h - 1)i$ ,  $0$ , and  $1$ ,  $h > 1$ . When  $h > 1$  we have by [10, pp. 103-104], [11]

$$(4.13) \quad \mathbf{M}(Q; 1 + hi, (h - 1)i, 0, 1) \equiv M(h) \equiv \mathcal{K}(r)/\mathcal{K}(r')$$

where

$$r = \left( \frac{t_1 - t_2}{t_1 + t_2} \right)^2, \quad t_1 = \mu_{1/2}^{-1} \left( \frac{\pi}{2c} \right), \quad t_2 = \mu_{1/2}^{-1} \left( \frac{\pi c}{2} \right), \quad c = 2h - 1.$$

Therefore, the quadrilateral can be conformally mapped onto the rectangle  $1 + iM(h)$ ,  $iM(h)$ ,  $0$ ,  $1$ , with the vertices corresponding to each other. It is clear that  $h - 1 \leq M(h) \leq h$ . The formula (4.11) has the following approximative version

$$M(h) = h + c + O(e^{-\pi h}), \quad c = -1/2 - \log 2/\pi \approx -0.720636,$$

given in [27]. As far as we know there is neither an explicit nor asymptotic formula for the case when the angle  $\pi/4$  of the trapezoid is replaced by an angle equal to  $\alpha \in (0, \pi/2)$ .

**4.14. Numerical computation of elliptic integrals.** The computation of the elliptic integrals is efficiently carried out by classical methods available in most programming environments (see [4] for details.) The same holds true for the hypergeometric functions. The numerical computation of  $\mu_{1/2}(r)$  and its inverse function can be carried out by standard procedures. See e.g. [4, 3.22, 5.32] and [20, 2.11].

## 5. VALIDATION OF ALGORITHMS: CONVEX QUADRILATERALS

Validation of the algorithms for the modulus of a quadrilateral will be discussed in two main cases: convex quadrilaterals and the case of a general polygonal quadrilateral. In this section the case of a convex quadrilateral will be discussed for the following three algorithms: (a) the SC Toolbox in MATLAB written by Driscoll [16], (b) the AFEM software due to Samuelsson [9], (c) the  $hp$ -method of the present paper implemented in the Mathematica language. The reference computation is carried out by the algorithm of [20], implemented in [20] in the Mathematica language (the algorithm  $\text{QM}[A, B]$  implementing the formula in Theorem 4.10). This implementation makes use of multiple precision arithmetic for root finding of a transcendental equation involving the hypergeometric function.

**5.1. Setup of the validation test.** All our tests were carried out in the same fashion using the reciprocal identity (4.3) and considering a quadrilateral with the vertices  $a, b, 0, 1$  with  $\text{Im } a > 0$ ,  $\text{Im } b > 0$ , and the line segments joining the vertices as the boundary arcs. The vertices  $b, 0, 1$  were kept fixed and the vertex  $a$  varied over a rectangular region in the complex plane. The numerical value  $b = -0.2 + i \cdot 1.2$  was used and the lower left (upper right) corner of the rectangular region was  $0.5 + i \cdot 0.2$  ( $1.5 + i \cdot 1.2$ ).

**5.2. The reference computation.** We used the Mathematica script of [20] for solving the equation in Theorem 4.10 for the computation of  $\text{QM}(a, b, 0, 1)$  in order to carry out the test. The conclusion was that the amplitude of the error was roughly  $10^{-17}$  i.e. there was practically no error. Note that the quadrilateral here is not always convex. On the basis of numerical experiments, it seems that the reference method does also work in non-convex cases, but this has not been rigorously proved.

**5.3. The SC Toolbox.** This test was carried out by a test program and the error was usually approximately  $10^{-9}$ .

**5.4. The AFEM package.** This test was carried out by the test program and the error was usually approximately  $10^{-10}$ .

**5.5. The *hp*-FEM software.** The test was based on the implementation of the *hp*-method due to the first author. The error was usually  $10^{-8}$  for  $p = 8$ ,  $10^{-11}$  for  $p = 13$  and  $10^{-14}$  for  $p = 20$ , using (0.15, 12)-meshes.

**5.6. Ranking of the methods.** The reference method gives by a clear margin the least error in the test setup. The next is the *hp*-method. The AFEM method is nearly as effective as the SC Toolbox.

## 6. VALIDATION: POLYGONAL QUADRILATERALS

In this section we will consider the validation of the algorithms for the modulus of a quadrilateral in the case of polygonal domains with  $q > 4$  vertices. In the case considered in the previous section there was a reference computational method, providing the reference value for the moduli. There is no similar formula available for the general polygonal case.

**6.1. Setup of the validation test.** All our tests were carried out in the same fashion as in the previous section, using the reciprocal identity (4.3). We selected a quadruple of points  $\{z_1, z_2, z_3, z_4\}$ , which is a subset of the set of vertices defining the polygon  $D$ , and assume that these are positively oriented. Thus  $(D; z_1, z_2, z_3, z_4)$  is a quadrilateral to which the reciprocal identity (4.3) applies.

**6.2. The notation  $\text{cmodu}(w, k_1, k_2)$  and  $\text{modu}(w, k_1, k_2)$ .** Suppose that  $w$  is a vector of  $p$  complex numbers such that the points  $w_1, \dots, w_q$ ,  $q \geq 5$ , are the vertices of a polygon  $D$  and that they define a positive orientation of the boundary. Choose indices  $k_1, k_2 \in \{1, \dots, p-1\}$  with  $k_1 < k_2$  and set  $z_1 = w_{k_1}$ ,  $z_2 = w_{k_1+1}$ ,  $z_3 = w_{k_2}$ ,  $z_4 = w_{k_2+1}$ . Then we define

$$\text{cmodu}(w, k_1, k_2) = \text{M}(D; z_1, z_2, z_3, z_4), \quad \text{modu}(w, k_1, k_2) = \text{M}(D; z_2, z_3, z_4, z_1).$$

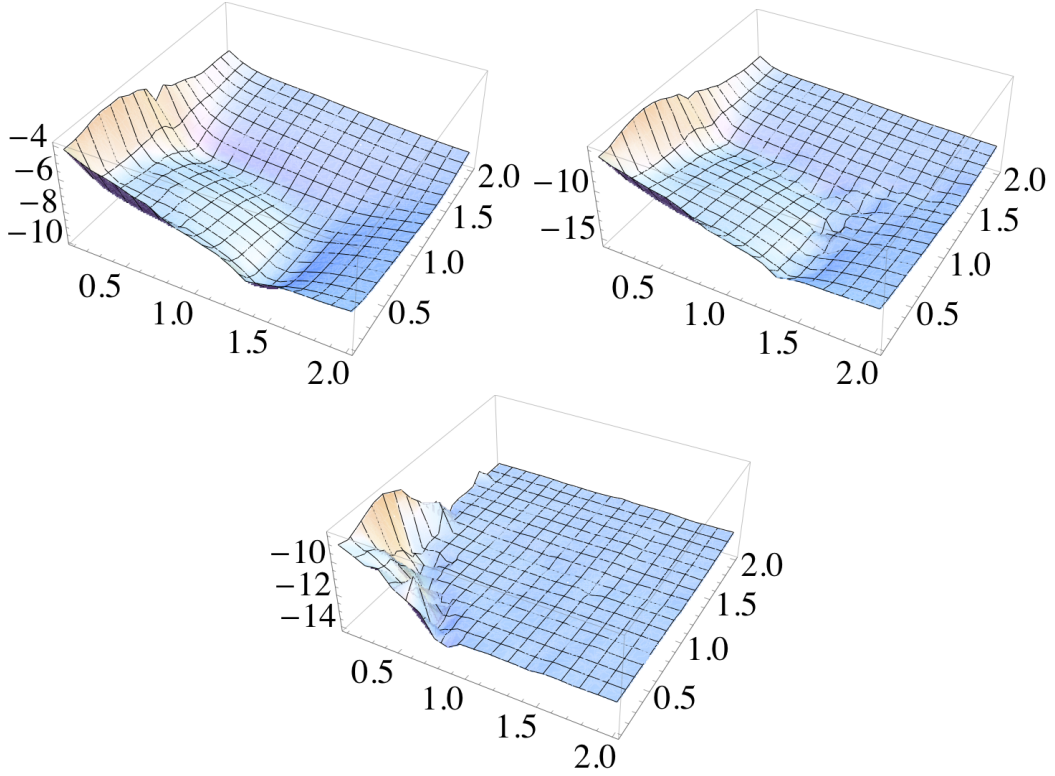


FIGURE 5. Logarithm of errors over the domain  $[0.1, 2] \times [0.1, 2]$ , corresponding to values of  $p = 8, 13, 20$  starting from above.

By the reciprocal relation (4.1) we have

$$(6.3) \quad \text{cmodu}(w, k_1, k_2) \cdot \text{modu}(w, k_1, k_2) = 1.$$

**6.4. L-shaped region.** The L-shaped region:

$$L(a, b, c, d) = L_1 \cup L_2, \quad L_1 = \{z \in \mathbb{C} : 0 < \text{Re}(z) < a, 0 < \text{Im}(z) < b\},$$

$$L_2 = \{z \in \mathbb{C} : 0 < \text{Re}(z) < d, 0 < \text{Im}(z) < c\}, \quad 0 < d < a, \quad 0 < b < c,$$

is a standard domain considered by several authors for various computational tasks. In the context of computation of the moduli it was investigated by Gaier [19] and we will compare our results to his results. In the test cases all the vertices had integer coordinates in the range  $[1, 4]$ .

**6.5. Tests of (6.3) with AFEM.** The error range was  $[-7.10 \cdot 10^{-10}, -1.80 \cdot 10^{-10}]$ .

**6.6. Tests of (6.3) with SC Toolbox.** The error range was  $[-1.37 \cdot 10^{-08}, 9.92 \cdot 10^{-09}]$ .

**6.7. Tests of (6.3) with  $hp$ -method.** The error ranges were for  $p = 12$ ,  $[4.0091 \cdot 10^{-11}, 1.58978 \cdot 10^{-10}]$ , for  $p = 16$ ,  $[8.03357 \cdot 10^{-13}, 2.28306 \cdot 10^{-12}]$ , and for  $p = 20$ ,  $[5.97744 \cdot 10^{-13}, 1.80145 \cdot 10^{-12}]$ , using (0.15, 12)-meshes.

## 7. RING DOMAINS

In this section, we compare  $hp$ -FEM with exact values and with AFEM in certain ring domains. The reference values are from [9].

**7.1. Square in square.** We compute here the capacity of the ring domain with plates  $E = [-a, a] \times [-a, a]$  and  $F = \mathbb{C}_\infty \setminus ((-1, 1) \times (-1, 1))$ ,  $0 < a < 1$ . The results with AFEM and the  $hp$ -method with  $(0.15, 12)$ -meshes are summarized in Table 1. For computation of the capacity, the ring domain is first split into four similar quadrilaterals. For the potential function, see Figure 7. Note that in this case, the exact values of the potential are known, see (4.13) and the related trapezoid type quadrilateral example.

**7.2. Cross in square.** Let  $G_{ab} = \{(x, y) : |x| \leq a, |y| \leq b\} \cup \{(x, y) : |x| \leq b, |y| \leq a\}$ . and  $G_c = \{(x, y) : |x| < c, |y| < c\}$ , where  $a < c$  and  $b < c$ . We compute the capacity of the ring domain  $R = G_c \setminus G_{ab}$ . The results with AFEM and the  $hp$ -method with  $(0.15, 16)$ -meshes are summarized in Table 2. For computation of the capacity, the ring domain is again first split into four similar quadrilaterals. The mesh for the quadrilaterals is given in Figure 6, and the potential function is given in Figure 7. The exact values are not known in this case but results can be compared with AFEM.

Since the underlying mesh topology remains constant in both examples above we have computed the results using exactly the same mesh template for every sub-problem, e.g. Figure 6 for Cross in square,  $a = 0.5, b = 1.2, c = 1.5$ . Thus, the results also measure the robustness of the method with respect to element distortion. Also, in both cases due to symmetry we have graded the mesh only to the reentrant corners of the domain.

TABLE 1. Table for Square in Square,  $p = 16$ 

<b>a</b>	Capacity	Error	Exact value
0.1	2.83978	$1.7 \cdot 10^{-9}$	2.8397774191
0.2	4.13449	$8.4 \cdot 10^{-12}$	4.1344870242
0.5	10.2341	$3.1 \cdot 10^{-12}$	10.2340925694
0.7	20.9016	$1.4 \cdot 10^{-10}$	20.9015816794
0.8	34.2349	$5.6 \cdot 10^{-13}$	34.2349151988
0.9	74.2349	$5.9 \cdot 10^{-10}$	74.2349151988

**Acknowledgments.** The authors are indebted to Prof. N. Papamichael for helpful comments on this paper.

TABLE 2. Table for cross in square,  $p = 16$ 

<b>a</b>	<b>b</b>	<b>c</b>	Capacity	Difference
0.5	1.2	1.5	21.9472192	$1.5 \cdot 10^{-8}$
0.5	1.0	1.5	14.0027989	$1.0 \cdot 10^{-8}$
0.2	0.7	1.2	9.1869265	$1.0 \cdot 10^{-8}$
0.1	0.8	1.1	11.2565821	$1.9 \cdot 10^{-8}$
0.5	0.6	1.5	7.3232695	$1.2 \cdot 10^{-8}$
0.1	1.2	1.3	23.1386139	$3.4 \cdot 10^{-8}$

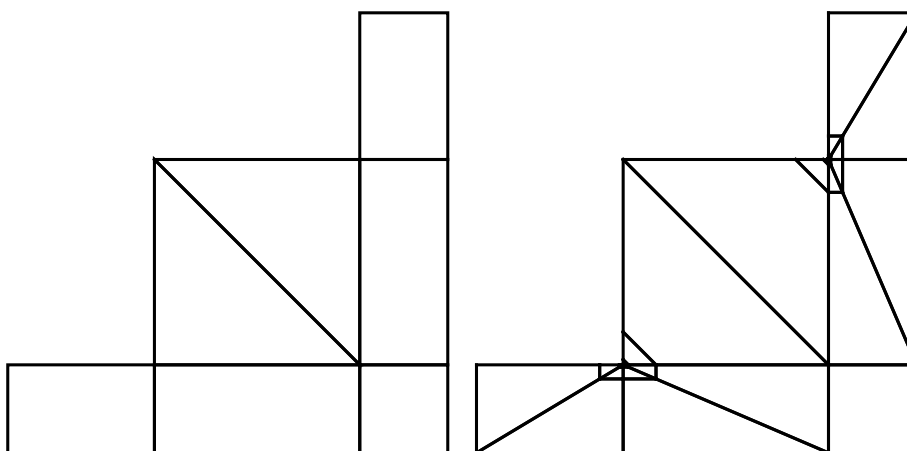


FIGURE 6. Meshing setup for cross in square

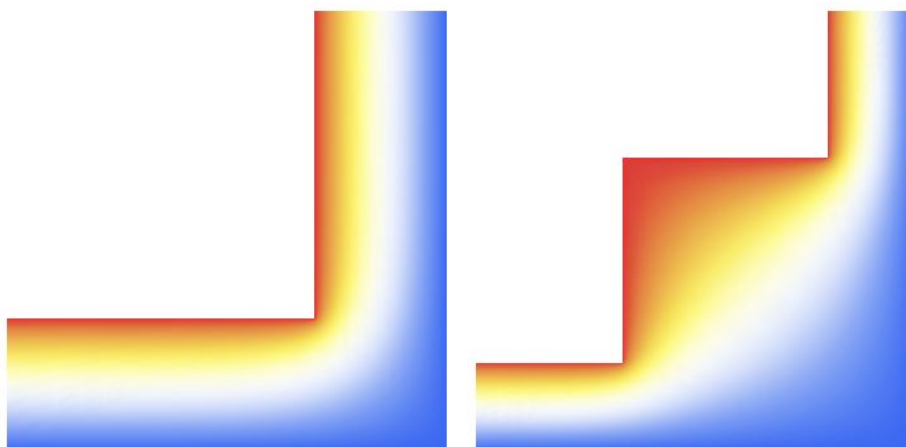


FIGURE 7. Potential functions: square in square and cross in square

## REFERENCES

- [1] L.V. AHLFORS, *Conformal invariants: topics in geometric function theory*. McGraw-Hill Book Co., 1973.
- [2] K. AMANO, *A charge simulation method for numerical conformal mapping onto circular and radial slit domains*. SIAM J. Sci. Comput. 19 (1998), no. 4, 1169–1187.

- [3] G.D. ANDERSON, S.-L. QIU, M.K. VAMANAMURTHY and M.VUORINEN, *Generalized elliptic integrals and modular equations*, Pacific J. Math. 192 No. 1 (2000), 1-37.
- [4] G.D. ANDERSON, M.K. VAMANAMURTHY and M. VUORINEN, *Conformal invariants, inequalities and quasiconformal mappings*, Wiley-Interscience, 1997.
- [5] I. BABUŠKA and M. SURI, *The P and H-P versions of the finite element method, basic principles and properties*, SIAM Review 36 (1994), 578-632.
- [6] L. BANJAI, *Revisiting the crowding phenomenon in Schwarz-Christoffel mapping*. SIAM J. Sci. Comput. 30 (2008), no. 2, 618–636.
- [7] I. BABUŠKA and B. GUO, *Regularity of the solutions of elliptic problems with piecewise analytical data, parts I and II*, SIAM J. Math. Anal., 19, (1988), 172–203 and 20, (1989), 763–781.
- [8] I. BABUŠKA and B. GUO, *Approximation properties of the hp-version of the finite element method*, Comp. Meth. Appl. Mech. Engr., 133, (1996), 319–346.
- [9] D. BETSAKOS, K. SAMUELSSON and M. VUORINEN, *The computation of capacity of planar condensers*, Publ. Inst. Math. 75 (89) (2004), 233-252.
- [10] F. BOWMAN, *Introduction to Elliptic Functions with applications*, English Universities Press Ltd., London, 1953.
- [11] W. BURNSIDE, *Problem of Conformal Representation*, Proc. London Math. Soc. (1) 24 (1893), 187-206.
- [12] D. CROWDY, *Geometric function theory: a modern view of a classical subject*, Nonlinearity 21 (2008), no. 10, T205–T219.
- [13] D. CROWDY and J. MARSHALL, *Constructing multiply connected quadrature domains*. SIAM J. Appl. Math. 64 (2004), no. 4, 1334–1359.
- [14] T. K. DELILLO, T. A. DRISCOLL, A. R. ELCRAT and J. A. PFALTZGRAFF, *Radial and circular slit maps of unbounded multiply connected circle domains*. Proc. R. Soc. Lond. Ser. A Math. Phys. Eng. Sci. 464 (2008), no. 2095, 1719–1737.
- [15] L. DEMKOWICZ, *Computing with hp-Adaptive Finite Elements, Vol. 1*, Chapman & Hall/CRC, 2006.
- [16] T.A. DRISCOLL, *Schwarz-Christoffel toolbox for MATLAB*, <http://www.math.udel.edu/~driscoll/SC/>
- [17] T.A. DRISCOLL and L.N. TREFETHEN, *Schwarz-Christoffel mapping*. Cambridge Monographs on Applied and Computational Mathematics, 8. Cambridge University Press, Cambridge, 2002.
- [18] V. DUBININ and M. VUORINEN, *On conformal moduli of polygonal quadrilaterals*. Israel J. Math. (to appear), arXiv math.CV/0701387
- [19] D. GAIER, *Conformal modules and their computation*, in ‘Computational Methods and Function Theory’ (CMFT’94), R.M.Ali *et al.* eds., 159-171. World Scientific, 1995.
- [20] V. HEIKKALA, M.K. VAMANAMURTHY and M. VUORINEN, *Generalized elliptic integrals*, Comput. Methods Funct. Theory 9 (2009), 75-109. arXiv math.CA/0701436.
- [21] P. HENRICI, *Applied and Computational Complex Analysis, vol. III*, Wiley, Interscience, 1986.
- [22] R. KÜHNNAU, *The conformal module of quadrilaterals and of rings*, In: Handbook of Complex Analysis: Geometric Function Theory, (ed. by R. Kühnau) Vol. 2, North Holland/Elsevier, Amsterdam, 99-129, 2005.
- [23] P.K. KYTHE, *Computational conformal mapping*. Birkhäuser, 1998.
- [24] D.E. MARSHALL and S. ROHDE, *Convergence of a variant of the zipper algorithm for conformal mapping*. SIAM J. Numer. Anal. 45 (2007), no. 6, 2577–2609.
- [25] N. PAPAMICHAEL, *Dieter Gaier’s contributions to numerical conformal mapping*, Comput. Methods Funct. Theory 3 (2003), no. 1-2, 1-53.
- [26] N. PAPAMICHAEL, *Lectures on Numerical Conformal Mapping*, <http://www.ucy.ac.cy/~nickp/numericalcn.htm>

- [27] N. PAPAMICHAEL and N.S. STYLIANOPOULOS, *The asymptotic behavior of conformal modules of quadrilaterals with applications to the estimation of resistance values*, Constr. Approx. 15 (1999), no. 1, 109–134.
- [28] R.M. PORTER, *An interpolating polynomial method for numerical conformal mapping*. SIAM J. Sci. Comput. 23 (2001), no. 3, 1027–1041.
- [29] R.M. PORTER, *History and Recent Developments in Techniques for Numerical Conformal Mapping*, Proceedings of the International Workshop on Quasiconformal Mappings and Their Applications (IWQCMA05), Dec 27, 2005- Jan 1, 2006, IIT Madras, edited by S. Ponnusamy, T. Sugawa, M. Vuorinen, (2007), 207–238, Narosa Publ Co, ISBN 81-7319-807-1.
- [30] R. SCHINZINGER and P. LAURA, *Conformal Mapping: Methods and Applications*, Elsevier, Amsterdam 1991.
- [31] CH. SCHWAB, *p- and hp-Finite Element Methods*, Oxford University Press, 1998.
- [32] E. SHARON and D. MUMFORD, *2D-Shape analysis using conformal mapping*, Intern. J. Computer Vision 70(1), 2006, DOI:10.1007/s11263-006-6121-z
- [33] B. SZABO and I. BABUŠKA, *Finite Element Analysis*, Wiley, 1991.
- [34] L.N. TREFETHEN, *Numerical computation of the Schwarz-Christoffel transformation*. SIAM J. Sci. Statist. Comput. 1 (1980), no. 1, 82–102.
- [35] L.N. TREFETHEN and T. A. DRISCOLL, *Schwarz-Christoffel mapping in the computer era*. Proceedings of the International Congress of Mathematicians, Vol. III (Berlin, 1998). Doc. Math. 1998, Extra Vol. III, 533–542.
- [36] R. WEGMANN, *Methods for numerical conformal mapping*, Handbook of complex analysis: geometric function theory. Vol. 2, (ed. by R. Kühnau), Elsevier, Amsterdam, 351–477, 2005.

*E-mail address:* harri.hakula@tkk.fi

INSTITUTE OF MATHEMATICS, P.O.Box 1100, FI-02015 HELSINKI UNIVERSITY OF TECHNOLOGY, FINLAND

*E-mail address:* antti.rasila@tkk.fi

INSTITUTE OF MATHEMATICS, P.O.Box 1100, FI-02015 HELSINKI UNIVERSITY OF TECHNOLOGY, FINLAND

*E-mail address:* vuorinen@utu.fi

DEPARTMENT OF MATHEMATICS, FI-20014 UNIVERSITY OF TURKU, FINLAND